Intrachain Dynamics of Large dsDNA Confined to Slitlike Channels

Jeremy J. Jones,[1] Johan R. C. van der Maarel,[2,3] and Patrick S. Doyle[1,2,*]

[1]*Massachusetts Institute of Technology, Cambridge, Massachusetts 02139, USA*

[2]*BioSystems and Micromechanics (BioSyM) IRG, Singapore-MIT Alliance for Research and Technology (SMART) Centre,
Singapore 117542, Singapore*

[3]*Department of Physics, National University of Singapore, Singapore 117542, Singapore*

Exploration of intrachain hydrodynamics of dsDNA within channels has been limited to indirect analysis of global coil dynamics. In this Letter, we isolate hydrodynamic interactions within single molecules of dsDNA confined to slitlike channels by making use of density covariance measurements. We show that the strength of hydrodynamic interactions in DNA is dependent on the intrachain correlation length and that screening by symmetry in slitlike confinement results in a screening length that is proportional channel height. Moreover, we directly show the partial draining nature of the blobs formed by dsDNA in slits and predict under what conditions a dsDNA blob should obey nondraining Zimm behavior.

Hydrodynamic interactions (HI) between particles within bounded domains has become a field of intense research because of its importance in colloidal sciences [1], polymer physics [2], and microfluidic applications. In free solution, long range solvent flow induced by particle motion decays as $1/r$, and the cooperative motion between particles is described by the Oseen-Burger tensor. If one confines the particle to a cylindrical pore (quasi-1D confinement) then the far field flow brought about by particle motion decays exponentially at lengths beyond the channel width. Hence, motion between particles due to solvent flow is decorrelated, and HI is said to be screened at lengths greater than the channel width [2,3]. However, many micro- or nanofluidic devices are more precisely described as quasi-2D or slit-like. Unlike the pore geometry, particle motion in slits induces a far field dipolar flow (Hele-Shaw flow) [4] which decays algebraically as $1/r^2$. Tlusty demonstrated that screening in an isotropic quasi-2D system is possible because the angular average over the disturbance velocity results in a many-body cancellation of HI [5]. Unlike exponential velocity decay in pores, there is no apparent screening length associated with the algebraic far field velocity decay in slits [6] and produces much uncertainty when developing theories of internal mechanics of confined polymers.

Traditionally, blob theory has been the foundation for describing intrachain dynamics of DNA confined to slitlike channels [7,8]. In this theory, dynamic lengths are naturally separated into lengths shorter and longer than the channel height h by assuming the polymer is composed of a string of blobs, each with diameter h. Expanding on work by Balducci *et al.* [9], Hsieh *et al.* [10] carefully examined each individual assumption of blob theory and concluded that HI between blobs is screened when dsDNA is confined to slits but that intrablob HI was weaker than proposed by blob theory (i.e., blobs are partial draining). Strychalski *et al.* [11] arrived

at a similar conclusion when analyzing their results for DNA diffusion in slits. Lin *et al.* compared the diffusion of circular and linear λ-DNA within slit channels [12]. They concluded that complete screening within a polymer coil occurs only when $h \ll R_{g,\text{bulk}}$; however, they fail to appreciate that contributions from HI vary at different lengths within the molecule. A more recent study by Lin *et al.* [13] maintains this viewpoint. Consider, for instance, how one determines the strength of intrachain HI using blob scaling for in-plane diffusivity, D. The original theory assumes $D \sim N^{-1}h^{2/3}$. The assumption of screening between blobs give rise to the N^{-1} factor and has been validated in previous experiments [9–12]. But, diffusivity power law dependence on h is a convolution of assumptions for the intrablob HI and chain static properties. Thus, experimental deviations from the original scaling cause uncertainty in regards to the nature of intrachain hydrodynamics. Moreover, this indirect method of measuring intrachain hydrodynamic interactions does not capture some of the underlying physics.

Here, we explore cooperative dynamics within single DNA molecules in slitlike channels using a two-point density correlation function [14]. This method allows us to isolate intrachain dynamics without varying channel height or molecular weight. It is shown that HI become decorrelated at length scales proportional to the channel height. This, to our knowledge, is the first time experiments have directly shown the existence of an effective HI screening length within slit channels. We are able to demonstrate that, for typical channel heights and solvent conditions, blobs are indeed partially draining. They are not Zimm-like, as is assumed in original blob theory. The degree of blob draining is shown to be dependent on the segmental concentration within individual blobs and hence is directly related to buffer conditions.

Equilibrium dynamics of λ-DNA (48.502 kbp, New England Biolabs) were studied in slit channels with heights

in the range from 90 nm to 2 μm. The DNA samples were
stained with YOYO-1 intercalating dye (Invitrogen) at 4
base pair per dye molecule and were immersed in a buffer
of $1.5 \times$ TBE (270 mM Tris base, 270 mM boric acid,
and 6 mM EDTA) with 4% β-mercaptoethanol (BME,
Cabiochem) and 0.1% (w/v) poly(vinylpyrrolidone)
(Polysciences). YOYO-1 dye locally untwists the double
helix causing the contour length to increase from ≈ 15 to
22 μm; however, the intrinsic persistence length has been
shown to be weakly dependent on the dye staining ratio
[15]. The buffer viscosity was measured as $\mu = 1.14$ cP,
and the ionic strength was estimated to be 56.9 mM.
An external dc power source was used to electrophorese
DNA into channels and subsequently turned off until the
molecules reached thermal equilibrium. Fluorescence exci-
tation was then turned on and video was captured using a
Hammamatsu EB-CCD camera (model 7190-43) at a rate of
30 frames per sec. The point spread function of our optical
system has a half-width maximum of 440 nm which allows
us to resolve two point correlations at a distance of 220 nm.
See Supplemental Material [16] for additional details.

The intensity distribution relative to the center of mass
for our 2D images, $I(\mathbf{r}, t)$, is related to the density covari-
ance function by

$$C(\mathbf{r}_1, \mathbf{r}_2, \delta t) = \langle \delta I(\mathbf{r}_1, t) \delta I(\mathbf{r}_2, t + \delta t) \rangle, \quad (1)$$

$$\delta I(\mathbf{r}, t) = I(\mathbf{r}, t) - \langle I(\mathbf{r}) \rangle, \quad (2)$$

where $\mathbf{r}_1$ and $\mathbf{r}_2$ are position vectors relative to the center
of mass and $\langle \rangle$ indicates an ensemble-averaged quantity.
Figure 1 shows example 2D images of λ-DNA molecules
in a 560 nm tall slit and the resulting $\langle I(\mathbf{r}) \rangle$. The dynamic
structure factor is related to a lower-dimensional projection
of the function

$$S(r, \delta t) = \sum_\theta \sum_\mathbf{R} C(\mathbf{R} + \mathbf{r}, \mathbf{R}, \delta t), \quad (3)$$

where $r = |\mathbf{r}|$ and θ defines orientation of the vector $\mathbf{r} =
r[\cos(\theta)\mathbf{e}_x + \sin(\theta)\mathbf{e}_y]$. The summations are taken over all
θ and position vectors, $\mathbf{R}$, within the image.

The function $C(\mathbf{r}_1, \mathbf{r}_2, \delta t)$ is not dominated by center-of-
mass translation at long times, and, therefore, it is an
excellent base for measuring intramolecular dynamic
response. Naturally, an important question is what are the
limitations of this technique? We are limited by our optics
to correlated motion on lengths larger than $r > 220$ nm.
Additionally, we are only able to measure long-time inter-
nal mechanics for $t > 33$ ms. Thus, motions dominated by
stretching modes and hydrodynamics are readily observed
while dynamics from bending undulations of dsDNA are
not (bending mode length, $r_{\text{bend}} \sim 2l_p \sim 100$ nm and
characteristic time, $\tau_{\text{bend}} \sim 10^{-5}$ s). When $S(r, \delta t)$ is
matched to a stretched exponential such as $S(r, \delta t) \propto
\exp[-(\delta t/\tau_r)^\beta]$, the stretching exponent β provides infor-
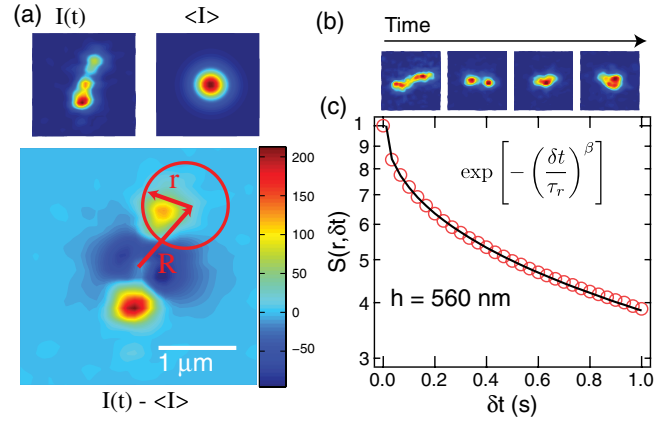mation about intracoil HI. From the de Gennes' dynamic

FIG. 1 (color online). Schematic of our analysis method for
extracting HI information within λ-DNA confined to a 560 nm
tall slit channel. (a) Example of an instantaneous 2D image with
intensity $I(t)$, the time average of all images $\langle I \rangle$ and visual
representation of the instantaneous intensity perturbation from
the average, $I(t)$-$\langle I \rangle$. The red arrows represent the position
vectors in $S(r, \delta t) = \sum_\theta \sum_\mathbf{R} C(\mathbf{R}, \mathbf{R} + \mathbf{r}, \delta t)$ and the circle in-
dicates the continuous integration over all θ. The analysis is done
for all time-varying images such as those in (b). Afterwards, we
perform a nonlinear regression with a stretched exponential
$S(r, \delta t) \propto \exp[-(\delta t/\tau_r)^\beta]$ as shown in (c).

light scattering models we expect $\beta_{\text{Rouse}} = 1/2$ [17,18] for
no HI and $\beta_{\text{Zimm}} = 2/3$ [18,19] for strong HI coupling.

Figure 2 shows the measured β as a function of varying
distance within λ-DNA under different degrees of confine-
ment. The shaded gray area represents our optical resolu-
tion limit and the horizontal dashed lines indicate the
Zimm and Rouse limits. A slit height of 2 μm weakly
confines λ-DNA ($R_{g,\text{bulk}} \approx 0.65$ μm) and, therefore, is
close to the free solution state. From this, one observes
that Rouse modes dominate the short distance dynamics
and Zimm behavior is prominent at long distances
($r > 1$ μm). This is in accord with results from Cohen
[14] and Shusterman [20] and demonstrates that HI domi-
nates the longest-time modes of λ-DNA *near equilibrium*.
We find at the strongest confinement conditions
($h = 90$ nm) the molecule exhibits purely Rouse-like dy-
namics suggesting complete screening of HI between DNA
segments. Bakajin *et al.* [21] made use of electrophoretic
force to stretch dsDNA in slit channels and, via numerical
modeling, implicitly showed negligible contribution of
HI at a channel height of 90 nm. At this height only one
Kuhn segment is within a blob of size $h = 2l_p \approx 100$ nm.
Therefore, the friction along individual Kuhn segments
dominates, and one observes Rouse dynamics.

The moderate confinement channels ($h = 1$ μm and
560 nm) provide more insight about the intrachain HI in
slits. The distance varying β curves show Rouse behavior
at short distances and a sub-Zimm β peak at intermediate
lengths. The apex is associated with the characteristic
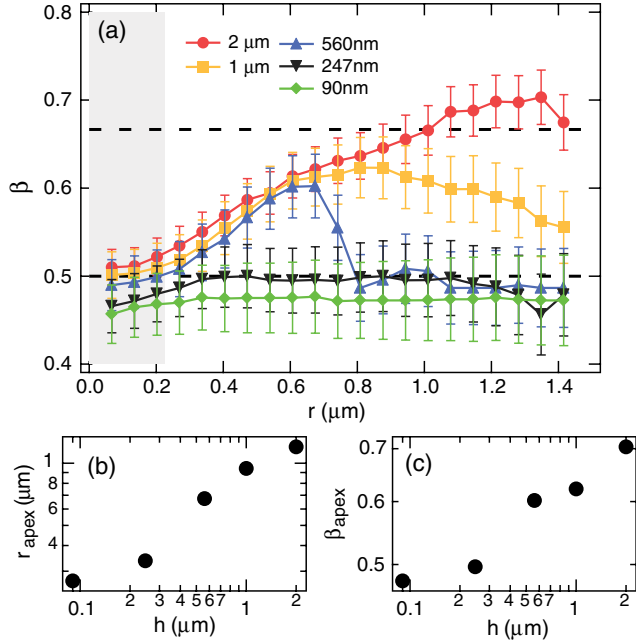length for the onset of HI screening and is directly related

FIG. 2 (color online).   (a) Summary of stretching exponent for the time-decay of the dynamic structure factor, $S(r, \delta t)$ for λ-DNA at variable channel heights. The horizontal dashed lines indicate Zimm ($\beta = 2/3$) and Rouse ($\beta = 1/2$) behavior. The grey shaded area represents the optical resolution limit, $r < 220$ nm. The lower graphs show the distance (b) r_{apex} at which the maximum value of (c) β_{apex} is attained for different channel heights.

to the channel height. At long distances the dynamics are Rouse-like indicating a screening of long range HI. We confirm that these channel heights are within the de Gennes regime, and, therefore, the behavior is not due to the crossover to an extended de Gennes state [22]. At intermediate distances in a quasi-2D system there will be transition in the solvent velocity decay from bulk (3D) to 2D. The regime where β decays from the apex to complete Rouse-like dynamics is indicative of this transition and the length over which β decays should theoretically scale with channel height.

As mentioned previously, experiments have shown that $D \sim N^{-1}$ for $h < R_{g,bulk}$ [9]. This scaling is indicative of intrachain hydrodynamic screening at lengths greater than h. From Tlusty's arguments for screening by symmetry [5] we may expect this long range screening effect. What is not clear from literature is the length scale over which such screening occurs. The peaks in β observed in moderate confinement may be thought of as being the draining characterization of a blob and an effective screening length at a particular channel height. We show in Figs. 2(b) and 2(c) the distance at which this apex in β is reached, r_{apex}, and the value of β_{apex} for each channel height. We simply choose the point at which β attains its maximum value or, for the case of the 90 nm channel, the

point where this β value plateaus. We define this plateau position as the location where β reaches within a relative error of 0.05 of its long distance average. As one reduces channel height, there is a reduction in the number of segments per characteristic blob resulting in a reduction in the strength of intrablob HI which explains the partial draining effect. This weakening of intrablob HI is also expected to manifest in scaling theory of the polymer's global dynamics. We measure the diffusivity, D, and longest relaxation time, τ, and confirm the scaling dependence with channel height (see Supplemental Material [16]). Experimental data from 90 nm to 1 μm channel heights result in a power law dependence of $D \sim h^{.49}$ and $\tau \sim h^{-.97}$ which is consistent with partially draining blobs [10]. From our data, we deduce that in channels of 2 μm or taller, one may apply classic blob theory (i.e., intrablob HI is Zimm-like). However, one must be able to create sufficiently long DNA molecules to have multiple blobs. DNA confined to a 2 μm tall slit and immersed in $1.5 \times$ TBE buffer would need to be nearly 90 μm long to form at least 2 blobs. After staining with YOYO-1, 4λ-DNA concatemers are approximately 88 μm long.

To test the effect of changing molecular weight, we have done experiments on the larger T4 DNA ($R_{g,bulk} \approx 1.33$ μm). Assuming that our DNA is moderately to strongly confined, we expect that the distance dependent HI effects to be independent of chain size. Figure 3(a) shows the results from this longer molecule, and Fig. 3(b) overlays the data from λ and T4 DNA molecules. The difference in measured β between the λ and T4 DNA data at any given distance is within 2%–5% of one another. T4 DNA is a larger molecule, and we are therefore able to measure β at longer distances. It is clear that screening of HI from channel walls occurs at lengths of $r > h$. Thus, for a given channel height, if one increases the DNA molecular weight the molecule will eventually attain an in-plane size such that the long distance dynamics are Rouse-like. Under the present solvent conditions, one may deduce that Zimm-like blobs are formed when the channel height is approximately 2 μm. However, the strength of intrablob HI will be dependent on the segmental density and the number of segments within each blob. Hence, one must also consider the effects of altering solvent conditions.

The strength of the dynamic interactions between two test particles in an unconfined Stokes flow may approximately be expressed as $E = \int H(r)g(r)dr$ [2], where $H(r)$ is the solvent velocity decay and $g(r)$ is the segmental pair correlation. To the first order, the pair correlation can be approximated by the segmental concentration, $g(r) \sim c$. Increasing polymer concentration magnifies the strength of HI within the DNA coil. The most direct method to alter the segmental concentration is to modulate the intrachain excluded volume. Experimentally, this involves changing the electrostatic screening between segments by varying the salt concentration. In Figure 4 we show results for
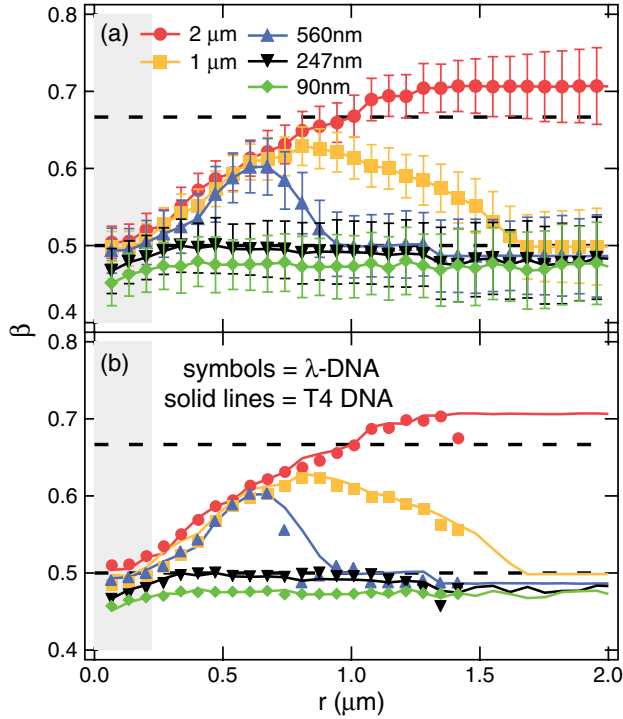
FIG. 3 (color online).   (a) Summary of stretching exponent for the time decay of the dynamic structure factor, $S(r, \delta t)$ for T4 DNA at variable channel heights. It is important to compare this data to the λ-DNA data as shown in (b). The solid markers are that of λ-DNA, and the solid lines are T4 DNA. The T4 DNA data extends further in r because the molecule is larger than λ-DNA.

FIG. 4 (color online).   (a) Time average intensity distribution, $\langle I \rangle$, of T4 confined to 1 μm slits in different ionic strength buffers. Notice, decreasing the ionic strength expands the in-plane size of the DNA coil. (b) Stretched exponential results for the T4 DNA in three different ionic strength buffers; 1.5 (56.9), 0.1 (5.3), and $0.02 \times$ TBE (1.5 mM).

measured β of T4 DNA confined to a 1 μm tall slit in three different buffers 1.5, 0.1, and $0.02 \times$ TBE with ionic strengths of 56.9, 5.3, and 1.5 mM, respectively.

Reducing the salt concentration enhances the excluded volume between segments thereby reducing the intrablob concentration. Consider an effective draining parameter, $h_{\mathrm{drain}} = N_{\mathrm{blob}} \gamma / (12\pi^3)^{1/2} \eta R$, for a blob [23]. We assume the blob size is equal to the channel height $R = h/2$, and the drag on each segment can be estimated as $\gamma \approx 6\pi\eta l_p / \ln(2l_p/d)$ (l_p = persistence length) [24]. The hydrodynamic width, $d = 2.76$ nm, is chosen to match free solution chain mobilities [25]. Modulation of the excluded volume changes the number of segments within the blob $N_{\mathrm{blob}} \approx h^{5/3} w^{-1/3} l_p^{-4/3}/2$ (w is the excluded volume segment width). Both l_p and w increase with decreasing ionic strength [26] (see Supplemental Material [16]). For $h_{\mathrm{drain}} \ll 1$ HI is weak, and for $h_{\mathrm{drain}} \gg 1$ HI is strong. Using this definition of the draining parameter we find the blob draining to be $h_{\mathrm{drain}} = 1.85$, 1.06, and 0.72 for blobs of size $R = h/2 = 0.5$ μm in 1.5, 0.1, and $0.02 \times$ TBE buffers, respectively. This indicates an increase in blob draining and is directly seen in Fig. 4. Long range, $r > h$, dynamics of confined DNA remain Rouse-like irrespective of ionic strength. Naturally, at the low salt limit,
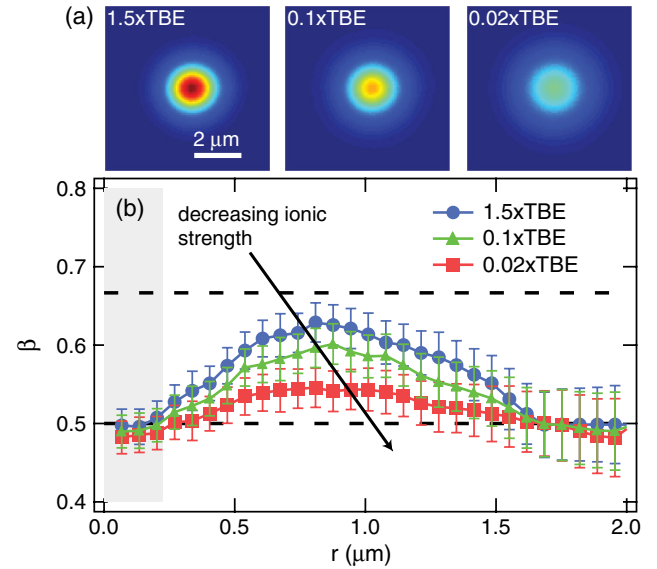
the intrachain concentration will be low enough to cause short length, $r < h$, dynamics to be fully Rouse, and, therefore, HI will be completely negligible within the confined coil.

In this Letter, we measured length dependent hydrodynamic cooperativity within single DNA molecules confined to slits. By isolating HI effects, we were able to show a HI screening length within slit channels that is proportional to the channel height. dsDNA has long served as a model polymer, but there has been recent suggestion that intrachain hydrodynamics will not dominant global chain dynamics for molecules of similar size to λ-DNA [27]. Here, we have shown that deviations in the current literature from blob theory can be explained by an insufficient length of contour composing each blob [10], and that, for moderate ionic conditions, the HI is dominant in blobs of radius $R \approx 1$ μm. These observations are of practical importance to microfluidic assays for DNA and bring to light the complexities of quasi-2D hydrodynamic flow fields in polymer physics.

*Corresponding author.
pdoyle@MIT.EDU

[1] R. Zangi and S. A. Rice, Phys. Rev. Lett. **92**, 035502 (2004).
[2] M. D. Graham, Annu. Rev. Fluid Mech. **43**, 273 (2011).

[3] H. Diamant, J. Phys. Soc. Jpn. **78**, 041002 (2009).

[4] N. Liron and S. J. Mochon, J. Eng. Math. **10**, 287 (1976).

[5] T. Tlusty, Macromolecules **39**, 3927 (2006).

[6] H. Diamant, B. Cui, B. Lin, and S. A. Rice, J. Phys. Condens. Matter **17**, S2787 (2005).

[7] F. Brochard and P. G. de Gennes, J. Chem. Phys. **67**, 52 (1977).

[8] M. Daoud and P. G. de Gennes, J. Phys. (Paris) **38**, 85 (1977).

[9] A. Balducci, P. Mao, J. Han, and P. S. Doyle, Macromolecules **39**, 6273 (2006).

[10] C.-C. Hsieh, A. Balducci, and P. S. Doyle, Macromolecules **40**, 5196 (2007).

[11] E. A. Strychalski, S. L. Levy, and H. G. Craighead, Macromolecules **41**, 7716 (2008).

[12] P.-K. Lin, J.-F. Chang, C.-H. Wei, P. H. Tsao, W. S. Fann, and Y.-L. Chen, Phys. Rev. E **84**, 031917 (2011).

[13] P.-K. Lin, C.-C. Hsieh, Y.-L. Chen, and C.-F. Chou, Macromolecules **45**, 2920 (2012).

[14] A. E. Cohen and W. E. Moerner, Phys. Rev. Lett. **98**, 116001 (2007).

[15] K. Günther, M. Mertig, and R. Seidel, Nucleic Acids Res. **38**, 6526 (2010).

[16] See Supplemental Material at http://link.aps.org/supplemental/10.1103/PhysRevLett.110.068101 for additional information on image acquisition, calculation dynamic structure factor and its relation to density-density covariance, and dsDNA electrostatic effects.

[17] P. G. de Gennes, Physics (Long Island City, N.Y.) **3**, 37 (1967).

[18] M. Doi and S. F. Edwards, *The Theory of Polymer Dynamics* (Oxford University Press, Oxford, 1998), p. 132.

[19] E. Dubois-Violette and P. G. de Gennes, Physics (Long Island City, N.Y.) **3**, 181 (1967).

[20] R. Shusterman, S. Alon, T. Gavrinyov, and O. Krichevsky, Phys. Rev. Lett. **92**, 048303 (2004).

[21] O. B. Bakajin, T. A. J. Duke, C. F. Chou, S. S. Chan, R. H. Austin, and E. C. Cox, Phys. Rev. Lett. **80**, 2737 (1998).

[22] L. Dai, J. J. Jones, J. R. C. van der Maarel and P. S. Doyle, Soft Matter **8**, 2972 (2012).

[23] B. H. Zimm, J. Chem. Phys. **24**, 269 (1956).

[24] J. Riseman and J. G. Kirkwood, J. Chem. Phys. **18**, 512 (1950).

[25] D. R. Tree, Y. Wang, and K. D. Dorfman, Phys. Rev. Lett. **108**, 228105 (2012).

[26] C.-C. Hsieh, A. Balducci, and P. S. Doyle, Nano Lett. **8**, 1683 (2008).

[27] F. Latinwo and C. M. Schroeder, Soft Matter **7**, 7907 (2011).